Colloids and Surfaces A: Physicochem. Eng. Aspects 489 (2016) 241–248

Contents lists available at ScienceDirect

Colloids and Surfaces A: Physicochemical and Engineering Aspects

journal homepage: www.elsevier.com/locate/colsurfa

Quantifying liquid drainage in egg-white sucrose foams by resistivity measurements

D. Daugelaite [a], R.-M. Guillermic [b], M.G. Scanlon [a,*], J.H. Page [b]

[a] Department of Food Science, University of Manitoba, Winnipeg, Manitoba R3T 2N2, Canada
[b] Department of Physics & Astronomy, University of Manitoba, Winnipeg, Manitoba R3T 2N2, Canada

HIGHLIGHTS

- The drainage properties and stability of egg-white sucrose foams are quantified.
- A new high-resolution AC conductance meter enables very accurate resistance measurements.
- The resistance measurements have improved resolution as a function of foam height compared with previous data.
- High gas volume fraction foams made from egg-white sucrose mixtures are shown to be very stable.
- Little drainage is evident in these foams even after 200 min.

GRAPHICAL ABSTRACT

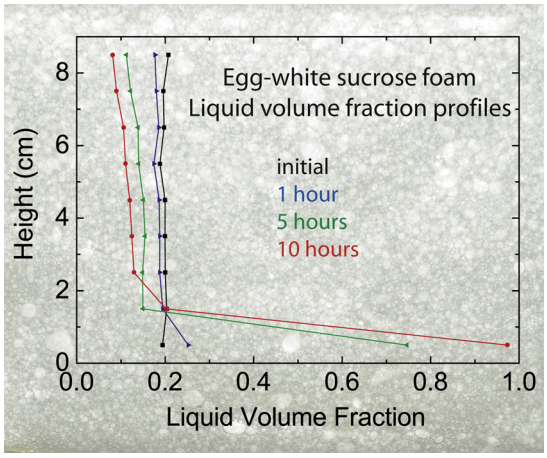

ARTICLE INFO

Article history:
Received 25 August 2015
Received in revised form 28 October 2015
Accepted 29 October 2015
Available online 2 November 2015

Keywords:
Free drainage analysis
Foam
Egg white
Aging

ABSTRACT

Free drainage in egg-white foams with a variety of gas volume fractions was investigated by an electrical resistivity technique. Changes in resistivity at different heights in the foam were monitored as a function of time thus giving information on the local liquid volume fraction (or content) and therefore the rate of foam drainage. The wettest egg-white foam was the most unstable, with changes in liquid volume fraction observed within minutes of foam aging. Because bubble sizes are very small, a huge effect of capillary forces confers egg-white foams with a very good stability to drainage. The complex nature of the egg-white liquid (bulk and interfacial properties), the likely presence of denatured-aggregate complexes in the Plateau borders, and very small bubble sizes are key parameters for understanding the stability of egg-white foams that makes them excellent foaming materials for food science and culinary purposes.

1. Introduction

Bubbly liquids and foams elicit a great deal of scientific interest because of their unusual properties [1–3]. Bubbly liquids consist of unpacked dispersions of bubbles in liquid, while foams are highly packed structures of bubbles. In a foam, bubbles packed

* Corresponding author.
E-mail address: Martin.Scanlon@umanitoba.ca (M.G. Scanlon).

http://dx.doi.org/10.1016/j.colsurfa.2015.10.053
0927-7757/

together form an interconnected structure, composed of films, Plateau borders and nodes. Because of this mechanical structure, foams can exhibit elastic, plastic or viscous behavior depending on the mechanical solicitation, contrary to bubbly liquids whose properties remain more liquid-like in character. The mechanical properties of foams are strongly linked to the bubble size distribution and the liquid volume fraction [4].

As well as being of scientific interest, bubbly liquids and foams are of substantial technological interest and value. For example, solid foams, created from solidification of liquid foams, are useful in a variety of mass-sensitive applications where their high ratios of modulus and strength relative to mass confer a number of performance advantages [5]. Liquid foams have a number of purposes in the petroleum industry [6], in fire-fighting technologies [7], and numerous foam fractionation applications are evident in the chemical processing industries [8,9]. Liquid foams are also of great interest in the cosmetic industry [7].

Bubbly liquids also prove their utility in industrial processes, particularly for mass transfer applications [10,11]. Their interesting nature is also exploited in biology, bubble clouds that enhance biomedical ultrasonic imaging techniques being one example [12,13], while the generation of bubble clouds by killer whales for corralling prey is an interesting example from nature [14]. Another biological application is in the kitchen and in commercial food production because aerated and foamed food products (e.g., wafers, meringues, angel food cakes, soufflés) are highly valued and popular products due to their capacity to create soft textures and appealing mouth feel [15–17].

Until solidification of the liquid matrix material, the structures of both foams and bubbly liquids are prone to significant changes over time [1,2,18–21]. These “aging” changes in aerated systems can be divided into two categories: aging by coarsening (disproportionation and coalescence) and aging induced by gravity.

Disproportionation and bubble coalescence are processes inducing an average bubble size growth with time. In foams both mechanisms occur, whereas in bubbly liquids disproportionation is the only mechanism. Disproportionation is driven by Laplace pressure differences that exist between bubbles of different sizes. The diffusion of gas from the smaller bubbles, where it is at a higher pressure, leads to a coarsening process where the median bubble size grows steadily over time [22,23]. Coalescence is the event where the liquid film separating adjacent bubbles in a foam thins so much that it catastrophically breaks down [19,24–26]. The rate of coalescence depends on bubble geometry and film drainage time, but also on an additional stochastic parameter, the probability of a rupture event per unit time and per unit surface area of the films [24–26].

Both foams and bubbly liquids undergo gravity-driven aging processes: creaming in the case of a bubbly liquid, drainage in the case of foam. In gravity-driven aging processes, the large density differences between the dispersed gas phase and the liquid matrix material causes bubbles to cream in bubbly liquids, except in very high viscosity matrices such as reactive polyurethane systems [27] and dough [28]. In foams, bubbles are locked in place by their neighbors [2] so that creaming does not occur. Instead, because of gravity, the liquid contained in the foam flows downward through the network of Plateau borders and nodes permeating the structure of the foam [19,21].

In foams the extent to which a particular aging mechanism dominates foam destabilization depends considerably on the foam’s gas content. Indeed, the volume fraction of gas separates foams into two categories in terms of their rheological properties: wet foams and dry foams [1,2,19,21]. Wet foams are more prone to instability due to drainage, whereas in dry foams disproportionation is enhanced by the thin films separating the bubbles. Aging mechanisms very often impact each other; for instance, disproportionation can be accelerated by the effects of drainage [1,3,18,19].

Because changes in the structure of bubbly liquids and foams affect their end-use performance [16,17], or the way in which solidification occurs in the material [5,29], there is a need to understand aging mechanisms in order to control them. Egg-white sucrose foams are a classic food example to illustrate the challenges one faces in the kitchen and in industrial manufacturing facilities if one is to create a foam that has desirable end-use properties [15,30–33]. The challenge arises because the liquid foam is simultaneously undergoing drainage, disproportionation and coalescence, and these destabilization phenomena are enhanced as the temperature rises in the initial stages of baking (20–60 °C) [31]. Angel food cake made from such a foam is a good example, for if the cake batter is not optimally aerated, accelerated drainage due to lower liquid viscosity leads to cake failure [32]. Over-aeration accelerates the rate of disproportionation and coalescence, due to reduced separation between bubbles [1,2], again inducing cake failure. Therefore, it is important to understand instability mechanisms and quantitatively evaluate the aging process in foams used for cake making in order to advance and initiate new bakery formulations and cake-making technologies.

The objective of this paper is to study drainage-induced aging phenomena in egg-white foams of varying gas volume fraction, with a view to understanding aging mechanisms that affect the quality of the final product. The free drainage experimental design was based on a realistic angel food cake making process: the height of the experimental cell was approximately that of the pan height used for angel food cakes. To interpret mechanisms associated with the drainage process in egg-white foams, the specific properties of the egg-white foams were considered: small bubble size, nature of the proteins and their behavior in the foam network, the nature of the liquid-foam/air interfaces and the high interfacial viscosity. Analyzing the drainage behavior of the studied foam, we show that liquid flow in the foam network was very slow relative to small molecule surfactant foams typically used for foam drainage studies.

2. Experimental

2.1. Foam sample preparation and characterization

To make the base egg-white foams, a typical formulation was chosen that is suited for angel food cake [18,32,33], except that soft wheat flour, salt, and cream of tartar were omitted; the former to obviate changes in foam structure that would arise from flour addition, and the latter two, because as strong electrolytes, they would interfere with foam resistivity measurements. Accordingly, 83 g sucrose and 83 g of egg white were used for all experiments. Except for the highest gas volume fraction, where egg white was separated from fresh eggs, liquid egg whites (Innovatech, Winnipeg, MB) were used. Liquid egg whites were kept frozen at −20 °C until needed. Prior to each experiment, the liquid egg whites were defrosted at 4 °C for 12 h and then allowed to reach ambient temperature (22 °C). The liquid egg whites were then filtered through cheese cloth to remove particulates. Powdered sucrose of fine particle size (for ready dissolution) was bought in 1 kg bags (Rogers Sugar Ltd.).

A small scale domestic Kitchen Aid (Hobart Company, Model 4C, 200 W) variable-speed mixer with a stainless steel three-wire whip was used to create the foams. Initially, the sugar and egg whites were blended in a steel bowl at very low speed (speed 1) for 5 min to dissolve the sucrose. Afterwards, high speed mixing (speed 6) was used to occlude air into the mixture. Four high speed mixing times were chosen to obtain egg-white foams with gas volume fractions of 0.60, 0.65, 0.78 and 0.81. Gas volume fractions (ϕ) in the foams

were calculated from the measured density (ρ) values by using the relation:

$$\phi = 1 - \frac{\rho}{\rho_0} \quad (1)$$

where ρ_0 is the density of the egg-white sucrose blend prior to air incorporation. The density of the egg-white sucrose blend and the foams were measured by filling a cylinder of known volume and weighing it [18]. The standard error of a minimum three replications for the density measurements was 0.5–6%.

The viscosity of the egg-white sucrose blend as a function of frequency was obtained from an oscillatory shear analysis (0.01–100 Hz) and from shear wave reflectance measurements, both as described by Leroy et al. [34]. From these measurements, the viscosity was found to be 33 times the viscosity of water: η = 33 mPa s [20].

A steel spatula and spoon were used to load the egg-white foam sample into the cylinder in less than 5 min. The top of the cylinder was covered with plastic film to avoid moisture evaporation from the foam. Three replicate foams were made for each gas volume fraction.

Bubble sizes were determined with a microscope after the formation of the foam and regularly up to 40 min of aging [20], and then extrapolated to longer times to have an idea of the global evolution of the bubble size during the drainage experiments.

2.2. Foam resistivity measurement technique

Direct measurements of the electrical resistance of foams are challenging [35]. A number of different electrode configurations and sample cell geometries have been used over the last several years to investigate liquid drainage in foams through electrical resistivity measurements [35,and references therein]. Our approach was based on the apparatus of Barigou et al. [36], who used a cylindrical cell with a central electrode. Our cell was 7 cm in diameter and 15 cm in height, and was fabricated by firmly stacking together 15 stainless steel and 15 polyoxymethylene (Delrin) plastic rings (Fig. 1), with the cylindrical stack being placed on a flat polyoxymethylene bottom plate. The plastic and steel rings were alternated along the height of the cylinder, thereby isolating the steel rings physically and electrically. The structure was tightened up from the bottom to the top by using 4 steel rods external to the cylinder. To prevent leakage, the rings were sealed with silicone gel.

The stainless steel rings functioned as outer electrodes and a central rod, positioned in the cylinder's geometric centre, acted as the inner electrode. The rod size (6.4 mm diameter) was chosen after conducting preliminary experiments using KCl and NaCl electrolyte solutions with rods of different thicknesses to determine the optimum diameter. The optimization criterion was that the diameter should be sufficiently large that the electric field lines near the rod are not too closely spaced, so that the local electric field is small enough not to significantly perturb the foam structure.

The resistance of the foam at different heights in the cell was measured by applying a voltage of constant magnitude from an AC signal generator (GFG-8016G, Good Will Instruments) between the central electrode and each ring, and measuring the resulting current using current-to-voltage converters. The AC frequency was chosen to be 1 kHz. Each of the tabs attached to the 15 outer rings was connected to its own current-to-voltage converter, and their output voltages were hooked up to a data logger. The data logger consisted of a shielded I/O connector block (NI SCB-68) and a sixteen-channel analogue to digital converter (NI PCI-6229), allowing simultaneous acquisition of the signals from all rings, as well as the driving voltage applied to the central post of the resistivity cell. Data logging was controlled using LabVIEW (National Instruments, Austin, Texas, USA), which was programmed via post-processing of the acquired signals to display either resistance (from the in-phase signals) or capacitance (from the out-of-phase components) as a function of measurement time. For the results reported in this paper, only the resistance option was used. Signal averaging was used to improve the signal to noise and permit accurate resistance measurements. Since signals from each ring were recorded simultaneously, this instrument was able to monitor changes in foam resistance as a function of height even for fast-draining foams.

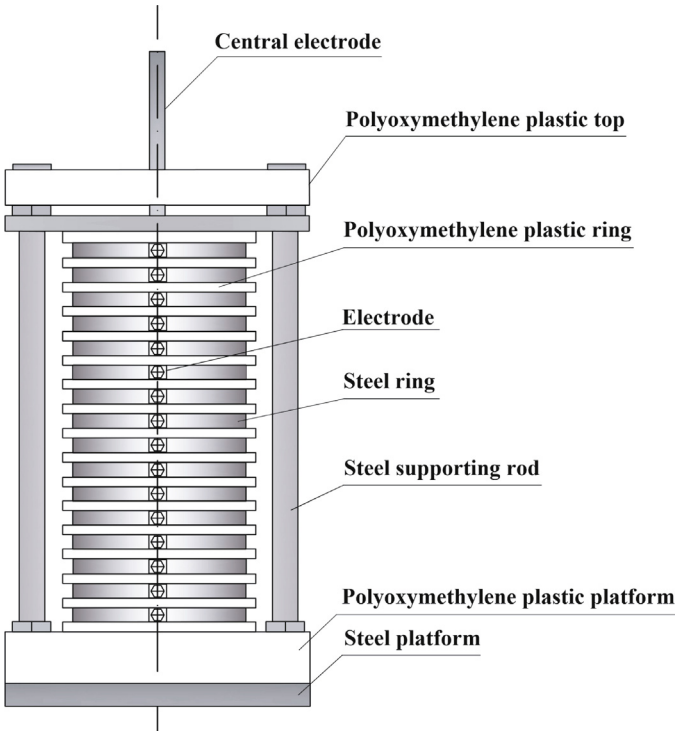

Fig. 1. Design of the cell for electrical resistivity measurements.

2.3. Current-to-voltage converter design

For accurate measurements of the electrical resistance as a function of height in the cylindrical cell, it is important that the electric field lines between the central electrode and the outer rings be straight and perpendicular to the electrodes, so that the region interrogated by each ring electrode be limited to a horizontal slice determined by the width of each ring. This was achieved in our cell through careful design of the current-to-voltage converters, which ensured that the inputs to the current-to-voltage converters connected to each ring were all at the same virtual ground. Thus, the rings on either side of each ring acted as guard rings, playing the same role as a guard ring in the perhaps more familiar parallel plate capacitor [37], so that straight field lines were established throughout the measurement volume, and the current flowing horizontally from the high-voltage central electrode to each ring could be accurately measured. The circuit diagram of the current-to-voltage converter for each ring is shown in Fig. 2. After converting current to voltage (Fig. 2, part B) and amplifying the signal 10 times (Fig. 2, part C), the resulting voltages were recorded by the data logger and used to determine the resistance of the foam, as described above. It should be emphasized that this design of the current-to-voltage converter enabled a significant improvement in the vertical resolution with which the resistance of the foam could be measured, and hence in the variation of the liquid volume fraction with height during drainage, compared with results using previous instruments.

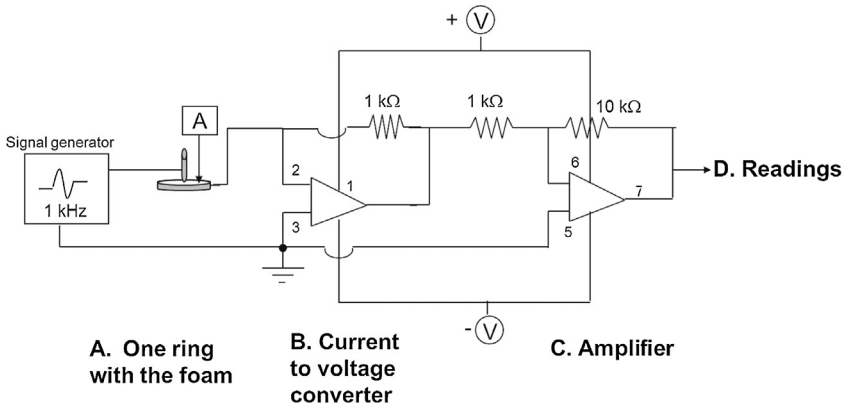

Fig. 2. Electrical circuit scheme of current meter-converter for a single ring in the cell.

To address the fact that the top and bottom rings did not have an effective guard ring above and below them, and as a result, the electric field lines of the top and bottom rings were not straight like the others, the measured voltages at the top and bottom rings had to be corrected by multiplying the measured values by a numerical constant. For the bottom ring, this numerical constant was 1.07, enabling accurate values of the resistance to be determined at this position as well. The value for this constant was determined experimentally from calibration measurements with salt solutions. Because of possible fluctuations in foam properties near the top of the foam during draining, data from the top electrode was not analyzed quantitatively, avoiding the difficulty of reliably determining the correction constant for the top electrode.

2.4. Electrical conductivity cell calibration

For calibration of the instrument, solutions of two strong electrolytes were chosen: NaCl and KCl. The concentrations (for KCl, 0.00745–0.3725 g/L, and for NaCl, 0.02–0.5 g/L) were selected so that their conductivities were in the same range as the conductivity of the foams. Conductivity values for the salt solutions were taken from the *CRC Handbook of Chemistry and Physics* [38]. The resistance (R) of the salt solution in the cell was calculated using Eq. (2) taking into account the cylindrical geometry:

$$R = \rho_R \int_{a_r}^{b_r} \frac{dr}{h(2\pi r)} = \frac{\rho_R}{2\pi h} \ln \frac{b_r}{a_r} \quad (2)$$

where ρ_R is the resistivity of the solution, b_r is the inner radius of the outer ring electrodes (3.5 cm), a_r is the radius of the inner electrode (0.32 cm), and h is the height of one ring (0.9 cm).

Calibration results for the KCl and NaCl solutions are shown in Fig. 3. The slopes show good agreement between measured and calculated conductivities of the salt solutions. The measured and calculated conductivity values of salt solution were slightly different for each ring. The ratio of calculated and measured KCl solution conductivity values of different rings were used to correct the measured foam conductivity values.

3. Results

3.1. Bubble size measurements

From microscopy measurements, the bubble radii (arithmetic average) for the $\phi = 0.78$ foams were initially found to be 12 μm and the evolution was shown to be very slow, reaching values close to 20 μm after 42 min of aging. By extrapolation to longer times, the radii were estimated to be close to 60 μm after 10 h of aging for the

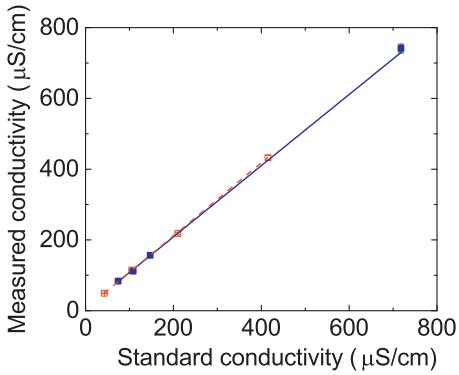

Fig. 3. Measured and standard conductivity of KCl (■) and NaCl (□) solutions. Lines represent linear fits to measured conductivity (slopes of 1.006 for KCl and 1.031 for NaCl).

$\phi_0 = 0.78$ foams. For the wetter foams with $\phi_0 = 0.65$, the bubble sizes were somewhat larger, starting around 18 μm and extrapolating to approximately 100 μm after 10 h. Thus, in egg-white sucrose foams, the bubbles are small and their sizes evolve very slowly—effects that have a profound influence on foam stability, as will be examined next.

3.2. Egg white foam resistivity and liquid volume fraction

Egg-white foam stability was evaluated by measuring the electrical resistance at different foam heights, thereby investigating the free drainage of liquid in the foam. All foam samples of four initial gas volume fractions (0.60, 0.65, 0.78, and 0.81) were 9 cm in height and remained at this height throughout the 600 min of aging time studied, meaning that the upper part of the foam does not coalesce with the external environment. Furthermore, microscopy observations of the foams during aging showed very few coalescence events between bubbles, indicating that coalescence was a negligible factor in this foam aging study. With the foam height of 9 cm, the lowest nine rings were covered with foam, so that data from eight rings were used in the measurements. To quantitatively evaluate changes in resistivity values, three foam height locations were chosen from the equally spaced locations, referred to as the bottom ($H = 0.5$ cm), middle ($H = 3.5$ cm) or top ($H = 7.5$ cm) of the foam. The resistivity change with aging time for two of the four different gas volume fraction foams at the different heights is displayed in Fig. 4. Error bars are small for the three replicates, typically smaller than the symbols used.

Egg-white foam stability varies according to the gas volume fraction (Fig. 4) with changes in foam resistivity being first manifest at

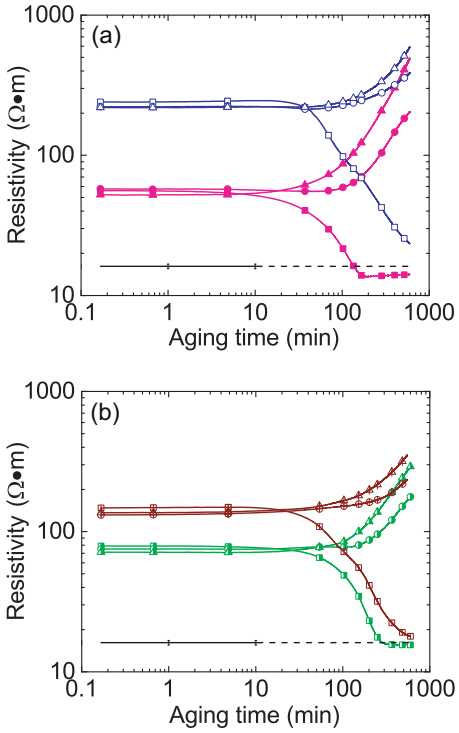

Fig. 4. Resistivity versus aging time for foams of four gas volume fractions (ϕ) at different foam heights. Measurements made at foam bottom (H = 0.5 cm) denoted by squares, in the middle (H = 3.5 cm) by circles, and at the top (H = 7.5 cm) by triangles. Horizontal line of low resistivity represents resistivity measurements of the egg white and sucrose mixture without air. (a) Foams of ϕ = 0.60 (solid symbols) and ϕ = 0.81 (open symbols). (b) Foams of ϕ = 0.65 (semi solid symbols) and ϕ = 0.78 (open symbols with vertical line). Error bars are comparable to or less than the size of the symbols in all cases, and therefore are not shown.

the bottom of the foam. For the wettest foam (ϕ = 0.60), changes in resistivity were evident by 30 min, while for the drier foams, changes in resistivity at different locations in the foam took longer. The foam located above the electrode where the measurement is performed acts as a reservoir of liquid, so the resistivity at this particular spot only starts to increase when the top layers of the foam have drained sufficiently. Capillary suction always maintains some liquid in the foam [19]. For the two wettest foams, after approximately 150 min and 450 min of aging, the resistivity of the bottom layer reaches approximately that measured in the egg-white liquid and sugar mixture containing no air (16.2 Ω m). Egg-white liquid evidently starts fully accumulating at the bottom of the foam so that at these longer aging times the measured resistivity is that of the egg-white liquid mixture. Slightly different resistivity values of the drained-out liquid reflect changes in the egg-white liquid and sucrose mixture: egg-white protein physicochemical structure is altered, and, in addition, protein composition in the drained liquid is likely to have changed [38–42]. As a consequence, the resistivity at a fixed spot on the foam column can vary in time not only because of a variation of the amount of liquid at this particular point but also because of a modification of the nature of the liquid.

The resistivity values of the middle and top parts of the foam increase continuously for all gas fraction foams with the foam resistance values of the top layer increasing at a faster rate. The differentiation in resistivity values with foam height is less pronounced at higher void fractions, indicative of the greater capillary forces to be overcome in the thinner network of Plateau borders of the higher gas fraction foams [43].

To quantify patterns of drainage in the foams as a function of time and foam height, it is desirable to convert resistivity values into liquid volume fractions [21,44,45]. From foam resistivity (ρ_r) values, the conductivity (σ) of the foam, which is inversely proportional to foam resistivity, was calculated. Using the conductivity of the egg-white/sucrose mixture with no air, σ_0, the relative conductivity, σ_r, was determined ($\sigma_r = \sigma/\sigma_0$). The initial liquid volume fractions (ϵ_0) of the foams (i.e., before drainage) were determined from initial gas volume fraction (ϕ_0) measurements using:

$$\epsilon_0 = 1 - \phi_0 \tag{3}$$

The initial gas volume fraction of the egg-white foams studied in this paper (81%, 78%, 65%, 60%) corresponds then to 19%, 22%, 35% and 40% liquid volume fraction foams. In Fig. 5 the measured relative conductivity (σ_r) values of the foams of different liquid volume fractions at zero min aging time (t = 12 s) are shown. At this time, minimal drainage has occurred (Fig. 4). Values plotted in Fig. 5 are the average of measurements of the foam from all eight rings (from 0.5 cm to 7.5 cm). As well, in Fig. 5 the relation between σ_r and ϵ derived by Feitosa et al. from foams made from small molecule surfactants with theoretical considerations of limiting values [46] is also shown for the full liquid volume fraction range, from 0 to 1:

$$\sigma_r = \frac{2\epsilon(1+12\epsilon)}{6+29\epsilon-9\epsilon^2} \tag{4}$$

From Fig. 5 it can be seen that the measured liquid volume fraction and the calculated one are in good agreement, showing that Feitosa et al.'s empirical relationship can be used in the case of complex protein foams. One can consider also another relationship using the tortuosity [47] that gives similar agreement.

$$\sigma_r = \frac{\epsilon}{\xi} \tag{5}$$

where ξ is tortuosity:

$$\xi = 1 - 0.5\ln(\epsilon) \tag{6}$$

Even though the tortuosity relation is not empirically derived, it is more difficult to use practically. For this reason, our liquid volume fractions as a function of time were determined by conductivity measurements using a form equivalent to Eq. (4) in terms of ϵ as a function of σ_r [46]:

$$\epsilon = \frac{3\sigma_r(1+11\sigma_r)}{1+25\sigma_r+10\sigma_r^2} \tag{7}$$

As the liquid volume fraction in the egg white foam decreases, a small discrepancy between the measured and calculated liquid volume fractions is apparent from Fig. 5: the liquid volume fraction in these foams is actually higher than values expected from relationships based on low molecular weight surfactant foams. This

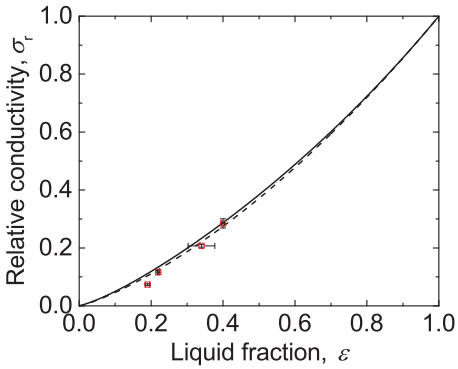

Fig. 5. Theoretical (lines) and measured (□) relative conductivity values versus liquid fraction for four egg-white sucrose foams. Relative conductivity relation of Feitosa et al. [46] (Eq. (4)) denoted with solid line, and relative conductivity with tortuosity model (Eq. (5)) [46] denoted with dashed line. Error bars represent standard deviation of three replicates of ϵ and σ_r measurements (some error bars smaller than symbol).

can be explained by the complex nature of the structure of egg-white proteins. Systems rich in proteins are capable of binding water or ions into their structure [48]. Plausibly, as the bubbles are formed in the foam, polypeptide chains are immobilized with water molecules at the air–water interface, limiting migration of ions and polyelectrolytes to some extent [48]. Protein denaturation, enhanced by the confinement in the films and Plateau borders, will also alter protein conductivity [44,49]. A second possible explanation is attributable to the small bubble size (radii from around 10 μm to roughly 100 μm after 600 min). For example, Datye and Lemlich [50] found that the measured relative conductivity was lower for foams with small bubbles in experiments on monodisperse foams of identical gas volume fraction but different bubble sizes. Because the Plateau border cross section dimensions do not decrease proportionally with decreasing bubble radius, differences in suction pressure in the Plateau borders can affect the relative conductivity [50].

3.3. Egg-white foam liquid volume fraction changes during aging—drainage study

The evolution of the liquid volume fraction (ϵ) at three different heights for the four egg-white foams is presented in Fig. 6. Far from the bottom of the foam, the liquid volume fraction decreases from its initial value. At the bottom of the foam, ϵ increases, indicating that the liquid progressively leaves the foam to form a pool of egg-white liquid. Because of the denaturation of the proteins at long times, the experiments were stopped before complete drainage of the foams occurred, after 10 h; foam stability at longer times is no longer relevant for the food science application envisaged. For surfactant foams, the decrease in the liquid volume fraction at a specific depth, z, can be captured by a power law at long drainage times [43,45]:

$$\epsilon(z) = \epsilon_o t^{\psi} \tag{8}$$

The exponent ψ in a classical surfactant foam depends on the mobility of the interfaces and on a parameter $\chi = (z/z_0)(t_0/t)^{0.5}$, taking into account the typical length scale z_0 (depth in the foam), and typical time t_0. Details of this model can be found in reference [45]. Usually ψ is between −1 and −2, −1 for immobile interfaces and −2 for mobile interfaces. For protein foams, foam composition is more complex and these established drainage models are not expected to apply; however, for the sake of comparison, it is still useful to see if the drainage behavior can be characterized by a power law, even if it is with very different exponents. In the particular case of egg-white sucrose foams, the slopes of the drainage curves at long times near the top of the foam are between −0.5 and −1, indicating very slow drainage, much slower than what is usually found for small molecular weight surfactant foams. Not far from the bottom of the foam, the liquid volume fraction decreases at an even slower rate, indicating a strong influence of capillarity.

Another way of visualizing the data is to consider liquid volume fraction profiles of the different foams studied. The evolution of the liquid volume fraction along the height of the column at different times and for different initial gas volume fractions (0.60 and 0.78) is shown in Fig. 7.

For the wettest foam (gas fraction 0.60), a variation of liquid volume fraction along the entire height is visible soon after the beginning of the experiment (around 10 min). For a given position along the column, the foam located higher up acts as a reservoir of liquid, so the decrease in the liquid volume fraction happens first at the top before occurring deeper in the foam. The overall liquid volume fraction in the foam decreases constantly, while the amount of liquid at the bottom increases. It is worth commenting that the liquid volume fraction measured in the drained egg-white liquid close

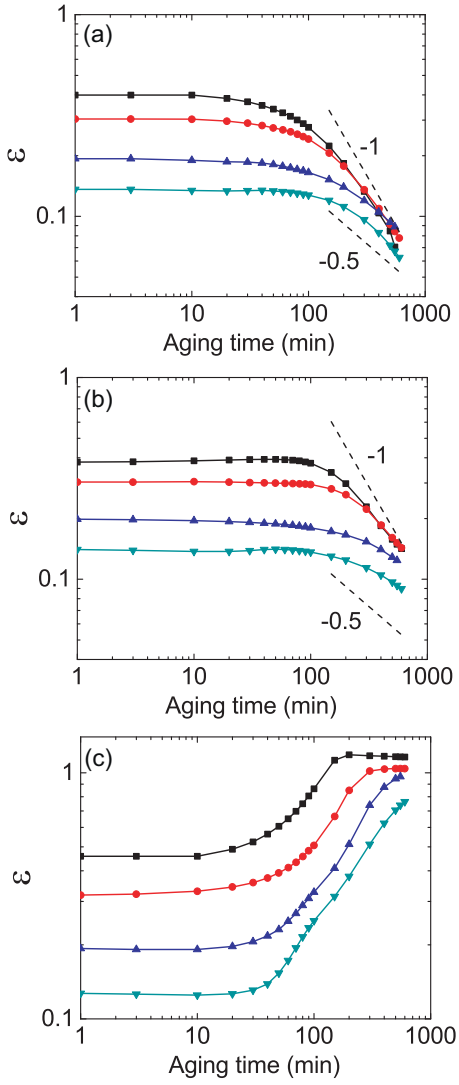

Fig. 6. Liquid fraction as a function of aging time for four different initial gas volume fraction foams: 0.60 (■), 0.65 (●), 0.78 (▲), 0.81 (▼). (a) at the 7.5 cm electrode, (b) at the 3.5 cm electrode, (c) at the 0.5 cm electrode. Dashed lines.

to the end of the experiment has a higher value than 1, indicating once again that the egg-white liquid at the beginning and at the end of the experiment are different, giving different conductivities. After 10 h of evolution, the foam is drier but did not totally drain and did not coalesce, showing the incredible stability of egg-white foams [30]. The drier foam (gas fraction 0.78) presents a slightly different drainage behavior: the liquid volume fraction is more or less constant over the entire height of the foam at all times, showing a slight curvature only after 200 min of aging. This amazing stability is probably a signature of the foam's strong capillarity due to the presence of very small bubbles, and of the nature of the egg-white sucrose mixture which has a higher viscosity than water and contains proteins and protein aggregates known to increase the foam's overall stability [51].

4. Discussion

All the egg-white foams studied show very slow drainage, much slower than the drainage of classic surfactant foams presented in the literature [44,49,52]. For surfactant foams, the exponent of the drainage curve indicates whether the interfaces are mobile or immobile, a mobile interface (plug flow) giving a slope of −2

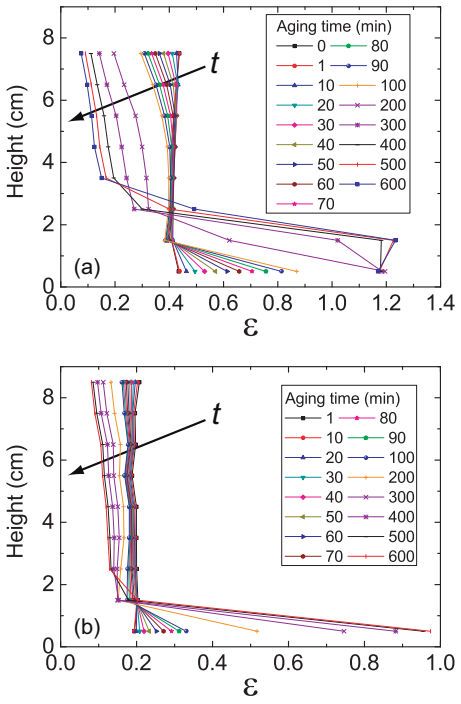

Fig. 7. Liquid fraction profiles for two different initial gas volume fractions: 0.60 (a) and 0.78 (b), at different aging times.

(fastest drainage) and an immobile interface (Poiseuille flow) a slope of −1. In the case of these egg-white foams, the slopes of the drainage curves at long times are between −0.5 and −1, indicating very slow drainage that cannot be described solely by the classic mobile/immobile interface descriptions. This behavior has been observed in other protein foams (for example [44,49]), supporting the idea that the slow rate of drainage is especially evident when protein aggregates are present. It is now accepted that protein foams can be considered to have immobile interfaces, leading to slow drainage rates [51]. This slow drainage behavior is further enhanced in high-sucrose egg whites where a number of proteins interact together in a limited free-water environment [52] so that such egg-white liquids are rather complex systems. The proteins of egg-white liquid undergo a surface-active conformational transition during the whipping process, with the mechanical treatment changing the structure of the proteins, so that albumin (the major foaming protein) is denatured to form a network structure [49,52–58]. Although these protein aggregates can reach the size of a few hundred nanometers and reduce foaminess, they do increase foam stability [49,58,59]. Regardless of whether the particles are purposely added [60,61] or formed during the foam making process, they reside in foam structure elements like the films and Plateau borders where they act as obstacles to liquid flow, thus reducing the drainage rate [62]. The wetter foams, having bigger Plateau border cross sections are less affected by these changes in protein structure; thus they drain faster than the drier foams, as expected.

In addition to this particular nature of the protein foam, the role of capillarity is also crucial. The bubbles in these foams are very small and their coarsening is very slow. The characteristic length, h_c, at which capillarity balances gravity is [19]:

$$h_c = \frac{l_c^2}{D} \tag{9}$$

with l_c the capillary length given by $l_c = \sqrt{\gamma/\rho g}$, where γ is the surface tension and g is the acceleration due to gravity. Therefore, the height over which the drainage is strongly influenced by the capillarity strongly depends on bubble diameter (D). This height will thus decrease when the bubble size increases. A rough estimation of h_c can be obtained, knowing the bubble size. Initially, the mean radius of the bubbles is around 10 μm, giving h_c = 21 cm. At 600 min, the mean bubble radius is between 60 μm and 100 μm depending on the initial liquid fraction of the foam studied, giving h_c = 3.5–2.1 cm. The height of the foam being 9 cm, capillarity cannot be neglected, and it explains well why the driest foams exhibit no significant drainage for more than an hour. Over the pool of liquid, ϵ is more or less constant over this height h_c, the foam acting as a "sponge" where the liquid is trapped due to capillarity.

5. Conclusions

Protein foam drainage is complex and distinct from surfactant foam liquid drainage. In the gas volume fraction range of 0.60–0.81, liquid drainage in egg-white foams is very slow. The bubble sizes of the egg-white foams are also very small at their creation leading to huge capillarity forces that helps the liquid to remain in the foam for a longer time. From what is already known for protein foams, we can expect that even at large heights in the foam where capillarity will not influence drainage as much, slow drainage will still be observed due to very rigid interfaces and aggregation of proteins. The drier egg-white foams have a remarkable stability over the height of the foam studied (9 cm), explaining why egg-white foams are such excellent systems for food applications.

Acknowledgements

Financial support for this research from NSERC Strategic and Discovery grants is very much appreciated, as is the donation of liquid egg-whites from John Thoroski (Innovatech, Winnipeg). We are also indebted to Kurt Hildebrand and Richard Hamel of the Physics and Astronomy Department at the University of Manitoba, who respectively designed and constructed the electrical measurement circuit for the resistivity cell.

References

[1] I. Cantat, S. Cohen-Addad, F. Elias, F. Graner, R. Höhler, O. Pitois, F. Rouyer, A. Saint-Jalmes, Foams Structure and Dynamics, Oxford University Press, New York, 2013.
[2] S. Weaire, D. Hutzler, The Physics of Foams, Oxford University Press, New York, 1999.
[3] G.M. Campbell, A history of aerated food, in: G.M. Campbell, M.G. Scanlon, D.L. Pyle (Eds.), Bubbles in Food 2: Novelty, Health and Luxury, Eagan Press, St. Paul, MN, 2008, pp. 1–22, AACC International.
[4] A.M. Kraynik, D.A. Reinelt, F. Swol, Structure of random foam, Phys. Rev. Lett. 93 (20) (2004), 208301.
[5] L.J. Gibson, M.F. Ashby, Cellular Solids: Structure and Properties, 2nd ed., Cambridge University Press, Cambridge, 1997.
[6] F. Schramm, L.L. Wassmuth, Foams: fundamentals and applications in the petroleum industry, Adv. Chem. Ser. 242 (1994) 3–45.
[7] R. Höhler, S. Cohen-Addad, Rheology of liquid foam, J. Phys. 17 (41) (2005) 1041–1069.
[8] R. Lemlich, Adsorptive bubble separation methods—foam fractionation and allied techniques, Ind. Eng. Chem. 60 (10) (1968) 16–29.
[9] S.T. Tobin, D. Weaire, S. Hutzler, Theoretical analysis of the performance of a foam fractionation column, Proc. R. Soc. A 470 (2014) 20130625.
[10] N. Kantarci, F. Borak, K.O. Ulgen, Bubble column reactors, Process Biochem. 40 (7) (2005) 2263–2283.
[11] Y.S. Cho, J.S. Laskowski, Effect of flotation frothers on bubble size and foam stability, Int. J. Miner. Process. 64 (2) (2002) 69–80.
[12] J.R. Lindner, Microbubbles in medical imaging: current applications and future directions, Nat. Rev. Drug Discov. 3 (6) (2004) 527–533.
[13] D. Cosgrove, Ultrasound contrast agents: an overview, Eur. J. Radiol. 60 (3) (2006) 324–330.
[14] T.G. Leighton, Nonlinear bubble dynamics and the effects on propagation through near-surface bubble layers, High Freq. Ocean Acoustics 728 (2004) 180–193.
[15] P. Barham, The Science of Cooking, Springer-Verlag, Berlin, 2001.
[16] Bubbles in Food, in: G.M. Campbell, C. Webb, S.S. Pandiella, K. Niranjan (Eds.), Eagan Press, St. Paul, MN, 1999.

[17] Bubbles in Food 2: Novelty, Health and Luxury, in: G.M. Campbell, M.G. Scanlon, D.L. Pyle (Eds.), Eagan Press, St. Paul, MN, 2008.
[18] J.E. Spencer, Examining the time-dependent changes in the bubble structure of whole egg and egg white foams and batters using small strain shear oscillatory rheology, large strain shear flow rheology and image analysis techniques, in: MSc Thesis, University of Manitoba, Canada, 2006.
[19] A. Saint-Jalmes, Physical chemistry in foam drainage and coarsening, Soft Matter 2 (10) (2006) 836–849.
[20] D. Daugelaite, Time dependent studies of foam stability using image analysis, electrical resistivity and ultrasound, in: PhD Thesis, University of Manitoba, Canada, 2011.
[21] S. Cohen-Addad, R. Höhler, O. Pitois, Flow in foams and flowing foams, Annu. Rev. Fluid Mech. 45 (1) (2013) 241–267.
[22] T. van Vliet, Physical factors determining gas cell stability in a dough during bread making, in: G.M. Campbell, C. Webb, S.S. Pandiella, K. Niranjan (Eds.), Bubbles in Food, Eagan Press, St. Paul, MN, 1999, pp. 121–127.
[23] M.B.J. Meinders, W. Kloek, T. van Vliet, Effect of surface elasticity on Ostwald ripening in emulsions, Langmuir 17 (13) (2001) 3923–3929.
[24] D. Monin, A. Espert, A. Colin, A new analysis of foam coalescence: from isolated films to three-dimensional foams, Langmuir 16 (8) (2000) 3873–3883.
[25] V. Carrier, A. Colin, Coalescence in draining foams, Langmuir 19 (11) (2003) 4535–4538.
[26] P.M. Ireland, Coalescence in a steady-state rising foam, Chem. Eng. Sci. 64 (23) (2009) 4866–4874.
[27] E. Mora, L.D. Artavia, C.W. Macosko, Modulus development during reactive urethane foaming, J. Rheol. 35 (5) (1991) 921–940.
[28] M.G. Scanlon, M.C. Zghal, Bread properties and crumb structure, Food Res. Int. 34 (10) (2001) 841–864.
[29] M. Nofar, B. Chul Park, Poly (lactic acid) foaming, Prog. Polym. Sci. 39 (10) (2014) 1721–1741.
[30] H. This, Solution to the whipped egg white challenge, Anal. Bioanal. Chem. 398 (5) (2010) 1845.
[31] M. Mizukoshi, Model studies of cake baking. IV. Foam drainage in cake batter, Cereal Chem. 60 (5) (1983) 399–402.
[32] E.J. Pyler, L.A. Gorton, Baking Science and Technology, vol. II, Sosland Publishing Company, Kansas, Merriam, 1988.
[33] J.E. Spencer, M.G. Scanlon, J.H. Page, Drainage and coarsening effects on the time-dependent rheology of whole egg and egg white foams and batters, in: G.M. Campbell, M.G. Scanlon, D.L. Pyle (Eds.), Bubbles in Food 2: Novelty, Health and Luxury, Eagan Press, St Paul, MN, 2008, pp. 117–129, AACC International.
[34] V. Leroy, K.M. Pitura, M.G. Scanlon, J.H. Page, The complex shear modulus of dough over a wide frequency range, J. Non-Newtonian Fluid Mech. 165 (9) (2010) 475–478.
[35] T.D. Karapantsios, M. Papara, On the design of electrical conductance probes for foam drainage applications: assessment of ring electrodes performance and bubble size effects on measurements, Colloids Surf. A 323 (1) (2008) 139–148.
[36] M. Barigou, N.S. Deshpande, F.N. Wiggers, An enhanced electrical resistance technique for foam drainage measurement, Colloids Surf. 189 (1) (2001) 237–246.
[37] R.F. Harrington, Introduction to Electromagnetic Engineering, Dover Publications, Mineola, NY, 2003.
[38] CRC Handbook of Chemistry and Physics, in: D.R. Lide (Ed.), 86th ed., CRC Press, 2005.
[39] L.R. MacDonell, R.E. Feeney, H.L. Hanson, The functional properties of egg white proteins, Food Technol. 9 (2) (1955) 49–53.
[40] F.E. Cunningham, Properties of egg white foam drainage, Poult. Sci. 55 (2) (1976) 738–743.
[41] P.J. Halling, Protein-stabilized foams and emulsions, CRC Crit. Rev. Food Sci. Nutr. 15 (2) (1981) 155–203.
[42] L. Bazinet, F. Castaigne, Y. Pouliot, Relative contribution of proteins to conductivity changes in skim milk during chemical acidification, Appl. Eng. Agric. 21 (3) (2005) 455–464.
[43] S.A. Koehler, S. Hilgenfeldt, H.A. Stone, A generalized view of foam drainage: experiment and theory, Langmuir 16 (15) (2000) 6327–6341.
[44] B. Rullier, B. Novales, M.A.V. Axelos, Effect of protein aggregates on foaming properties of β-lactoglobulin, Colloids Surf. A 330 (2) (2008) 96–102.
[45] A. Saint-Jalmes, D. Langevin, Time evolution of aqueous foams: drainage and coarsening, J. Phys. 14 (40) (2002) 9397–9412.
[46] K. Feitosa, S. Marze, A. Saint-Jalmes, D.J. Durian, Electrical conductivity of dispersions: from dry foams to dilute suspensions, J. Phys. 17 (41) (2005) 6301–6305.
[47] J.B. Yianatos, A.R. Laplante, J.A. Finch, Estimation of local holdup in the bubbling and froth zones of a gas-liquid column, Chem. Eng. Sci. 40 (10) (1985) 1965–1968.
[48] J.F. Zayas, Functionality of Proteins in Food, Springer-Verlag, Berlin, 1997.
[49] B. Rullier, M.A.V. Axelos, B. Langevin, D. Novales, β-Lactoglobulin aggregates in foam films: correlation between foam films and foaming properties, J. Colloid Interface Sci. 336 (2) (2009) 750–755.
[50] R. Datye, A.K. Lemlich, Liquid distribution and electrical-conductivity in foam, Int. J. Multiphase Flow 9 (6) (1983) 627–636.
[51] A.L. Fameau, A. Salonen, Effect of particles and aggregated structures on the foam stability and aging, Comptes Rendus Phys. 15 (8) (2014) 748–760.
[52] V. Raikos, L. Campbell, S.R. Euston, Effects of sucrose and sodium chloride on foaming properties of egg white proteins, Food Res. Int. 40 (3) (2007) 347–355.
[53] Y. Nakamura, Y. Sato, Studies on the foaming properties of the chicken egg white: Part IX. On the coagulated proteins under various whipping conditions (The mechanism of foaminess (1)), Agric. Biol. Chem. 28 (8) (1964) 524–529.
[54] L. Du, A. Prokop, R.D. Tanner, Effect of denaturation by preheating on the foam fractionation behavior of ovalbumin, J. Colloid Interface Sci. 248 (2) (2002) 487–492.
[55] C.K. Lau, E. Dickinson, Instability and structural change in an aerated system containing egg albumen and invert sugar, Food Hydrocolloids 19 (1) (2005) 111–121.
[56] T. Croguennec, A. Renault, S. Beaufils, J.J. Dubois, S. Pezennec, Interfacial properties of heat-treated ovalbumin, J. Colloid Interface Sci. 315 (2) (2007) 627–636.
[57] E. Dickinson, Food emulsions and foams: stabilization by particles, Curr. Opin. Colloid Interface Sci. 15 (1) (2010) 40–49.
[58] X. Yang, T.K. Berry, E.A. Foegeding, Foams prepared from whey protein isolate and egg white protein: 1. Physical, microstructural, and interfacial properties, J. Food Sci. 74 (5) (2009) E259–E268.
[59] J.P. Davis, E.A. Foegeding, Foaming and interfacial properties of polymerized whey protein isolate, J. Food Sci. 69 (5) (2004) C404–C410.
[60] A. Britan, M. Liverts, G. Ben-Dor, S.A. Koehler, N. Bennani, The effect of fine particles on the drainage and coarsening of foam, Colloids Surf. 344 (1) (2009) 15–23.
[61] R.M. Guillermic, A. Salonen, J. Emile, A. Saint-Jalmes, Surfactant foams doped with laponite: unusual behaviors induced by aging and confinement, Soft Matter 5 (24) (2009) 4975–4982.
[62] E. Dickinson, Structuring of colloidal particles at interfaces and the relationship to food emulsion and foam stability, J. Colloid Interface Sci. 449 (2015) 38–45.